Multicellular spheroid formation and evolutionary conserved behaviors of apple snail hemocytes in culture

Juan A. Cueto, Israel A. Vega, Alfredo Castro-Vazquez*

Laboratory of Physiology (IHEM-CONICET), Department of Morphology and Physiology (FCM-UNCuyo), Casilla de Correo 33, 5500 Mendoza, Argentina

ARTICLE INFO

ABSTRACT

A hemocyte primary culture system for *Pomacea canaliculata* in a medium mimicking hemolymphatic plasma composition was developed. Hemocytes adhered and spread onto culture dish in the first few hours after seeding but later began forming aggregates. Time-lapse video microscopy showed the dynamics of the early aggregation, with cells both entering and leaving the aggregates. During this period phagocytosis occurs and was quantified. Later (>4 h), hemocytes formed large spheroidal aggregates that increased in size and also merged with adjacent spheroids (24—96 h). Large single spheroids and spheroid aggregates detach from the bottom surface and float freely in the medium. Correlative confocal, transmission electron and phase contrast microscopy showed a peculiar organization of the spheroids, with a compact core, an intermediate zone with large extracellular lacunae and an outer zone of flattened cells; also, numerous round cells emitting cytoplasmic extensions were seen attaching to the spheroids' smooth surface. Dual DAPI/propidium iodide staining revealed the coexistence of viable and non-viable cells within aggregates, in varying proportions. DNA concentration increased during the first 24 h of culture and stabilized afterward. BrdU incorporation also indicated proliferation. Spontaneous spheroid formation in culture bears interesting parallels with spheroidal hemocyte aggregates found *in vivo* in *P. canaliculata*, and also with spheroids formed by tumoral or non-tumoral mammalian cells *in vitro*.

1. Introduction

Pomacea canaliculata is a highly invasive freshwater snail original from the Plata river basin [1], which has become a serious threat to rice and other crops in Asia and some Pacific islands [2—4]. Also, it has been found associated to outbreaks of eosinophylic meningoencephalitis, an emergent parasitic disease [5,6]. Beyond these applied aspects, basic studies on this species have revealed amazing aspects of its biology, for instance the first records of nuptial feeding behavior in a mollusk [7] and of egg proteins being either neurotoxic or antidigestive in animals [8,9]. Knowledge of the biology of this snail in general, and particularly of its immune system, may provide cues for understanding its apparent 'tolerance' to multiple symbiotic associations [10] and perhaps for controlling its populations [11].

Mollusks express innate (but not adaptive) immune reactions to microbes and parasites, and hemocytes are involved in these reactions as well as in wound healing [12]. Hemocytes share certain features with macrophages, their counterpart in the vertebrate immune system [13,14]. Among these are the capacities of phagocytosis, encapsulation and lysis of foreign cells [15]. Although there is abundant information on the defense mechanisms in some mollusk taxa [16], experimental studies have been frequently hampered by the scarcity of adequate *in vitro* model systems, which are just a few in gastropods [17—19].

Comparative studies of gastropod hemocytes have revealed a diversity of morphological types differing mainly in nuclear shape and location, nuclear/cytoplasmic ratio, emission of pseudopodia, and properties of cytoplasmic granules, but have been made mainly in pulmonates [e.g., 20—23]. Information on hemocyte morphology in *P. canaliculata* is limited, but three cell types can be recognized: (1) agranulocytes, unfrequent cells only discernable under transmission electron microscopy, which show a high nuclear/cytoplasmic ratio, and few or none cytoplasmic granules of moderate electron density; (2) granulocytes with a small nuclear/cytoplasmic ratio, and numerous, large electron-dense granules, which are eosinophilic in light microscopy preparations; and (3) hyalinocytes,

with an intermediate nuclear/cytoplasmic ratio and no apparent granules under light microscopy, but which show some granules of moderate electron density, and also electron-lucid spaces which probably represent glycogen accumulation [24–26].

In this study, a primary culture system for *P. canaliculata* hemocytes was developed, in which the evolutionary conserved processes of cell attachment, spreading and phagocytosis were observed shortly after seeding, but which were later followed by a remarkable formation of three-dimensional aggregates.

2. Material and methods

2.1. Animals, hemolymph sampling and cell counting

Adult snails of a cultured strain of *P. canaliculata* [27] were used. Hemolymph (1–2 mL per snail) was obtained by puncturing the heart ventricle, through a small opening made in the shell near the umbilicum, and through the underlying mantle and pericardium, using a sterile 25-gauge needle on a 1 mL syringe. Hemocyte concentration was determined in freshly extracted hemolymph, which was diluted (1:4) in an antiaggregant solution designed for *P. canaliculata* (30 mM EDTA, 43 mM NaCl, 1.8 mM KCl, 10 mM HEPES, pH 7.6) and cells were counted in a Neubauer hemocytometer. Hemolymph smears were stained with May-Gründwald-Giemsa to determine the percent of hyalinocytes and eosinophilic granulocytes.

2.2. Culture media

The basic medium was prepared from a stock solution containing 10 mL RPMI 1640 vitamins solution (100×, Sigma–Aldrich, R7256),

20 mL RPMI 1640 amino acids solution (50×, Sigma–Aldrich, R7131), 5.5 mmol glucose, 43 mmol NaCl, 1.8 mmol KCl, 4.25 mmol CaCl$_2$, 10 mmol 4-(2-hydroxyethyl)-L-piperazine-ethanesulfonic acid (HEPES), 0.026 mmol phenol red made up to 1 L in double distilled water; pH was adjusted to 7.6 with 3 M NaOH to which 25 mL of 82 mM L-glutamine, and 5 mL of a penicillin and streptomycin solution (10^7 IU/L and 50 mg/L, respectively) were added before use (the addition of the latter components tended to lower the medium pH to 7.45). This basic medium was supplemented in some experiments with fetal calf serum (10%) or homologous hemolymph plasma (15%). Also, a 1:1 dilution of the L-15 medium (GIBCO) was used when indicated, and was prepared by with distilled water to approximate the osmolarity of *P. canaliculata* internal milieu (Cueto et al., 2011).

2.3. Primary culture of hemocytes

Freshly extracted hemolymph (200 μL, approximately 6×10^5 cells per well) was seeded in a 24-well plate (Nunclone™ surface, Nunc™, Denmark), and each well was provided with 0.5 mL of the culture medium, and with (or without depending on the assay requirement) a bottom glass coverslip. Cells were allowed to settle and attach to the bottom coverslip or directly to the culture dish for 15 min and were then maintained at 28 °C for 0, 24, 48, 72 or 96 h unless otherwise indicated.

2.4. Phagocytosis assay

Hemocytes were seeded as described in Section 2.3. After 15 min, the medium was replaced by a 0.5 mL suspension of fluorescent latex beads (Fluoresbrite YG Microspheres, 1 μm; Polysciences Inc.)
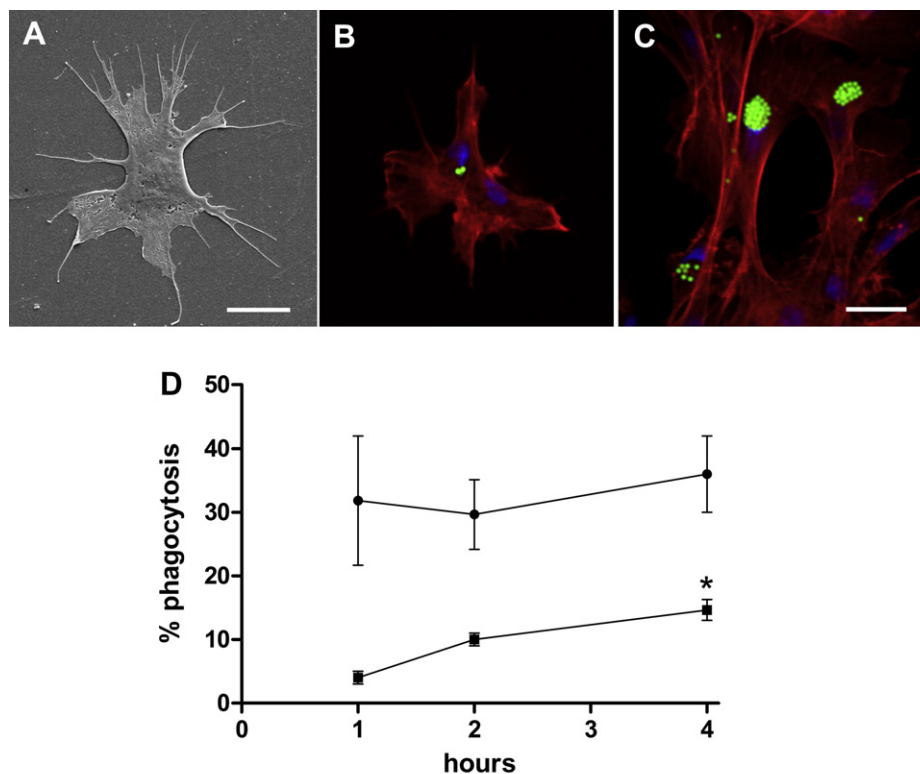

Fig. 1. Hemocytes of *Pomacea canaliculata* 15 min after seeding in the basic medium. A. Attached hemocyte with long filopodia (scanning electron microscopy). B. Phagocytic hemocytes; nuclei are blue (Hoechst 33258), actin is shown in red (rhodamine-labelled phalloidin) and fluorescent latex beads are green (laser confocal microscopy). Two hemocytes that have engulfed more than 20 fluorescent latex beads are shown. Scale bar = 10 μm. D. Percent of phagocytic hemocytes at different times after exposure to latex beads. The percent of hemocytes that had phagocytosed at least one bead remained constant (●), but the percent of hemocytes showing more than 20 phagocytosed beads (■) showed a statistically significant increment at 4 h (asterisk; one-way ANOVA and Tukey test as *post hoc* analysis). (For interpretation of the references to colour in this figure legend, the reader is referred to the web version of this article.)

in the basic medium, to assess the hemocyte phagocytic ability (the bead:hemocyte ratio was approximately 10:1). Hemocytes were incubated with latex beads for 1 h, 2 h and 4 h. Cells were then fixed in 2% (w/v) paraformaldehyde for 15 min at room temperature and stained with rhodamine conjugated phalloidin as follows: After three washes in phosphate buffer-saline, cells were permeabilized in 0.2% (v/v) Triton X-100 for 5 min, washed and then stained with rhodamine conjugated phalloidin (0.1 mg/mL in phosphate buffer-saline) for 60 min in the dark at room temperature. Cells were also treated with Hoechst 33258 for DNA staining, mounted in Mowiol and examined under an Olympus FV1000 laser confocal microscope.

Phagocytosis was quantified as the percent of hemocytes that have engulfed one or more fluorescent beads. Multiple comparisons ($n = 3$ per group) were made by one-way ANOVA followed by a Tukey test ($\alpha = 0.05$).

2.5. Assessment of hemocyte growth

For cell growth assessment, cultures were stopped by cooling at the preceding time periods and cells were detached with a rubber scraper and the medium containing cells was removed by pipetting. Then, cells were harvested by soft centrifugation ($100\times$ g, 10 min, 4 °C) and were sonicated with a microtip (three 15 s ultrasound exposures, with 25 s intervals in an ice bath; Kontes 100 W Ultrasonicator, Vineland, NJ, USA) in 0.2 mL of a high-salt buffer (Tris–HCl 100 mM, EDTA 10 mM, NaCl 2 M, pH 7.4) to ensure chromatin dissociation. DNA content of the sonicates was determined by the method of Labarca and Paigen [28]. Multiple comparisons ($n = 6$ per group) were made by one-way ANOVA followed by a Tukey test ($\alpha = 0.05$), after testing normality with the Kolmogorov–Smirnov test.

One pulse of 10 μM 5-bromo-2′-deoxy-uridine (BrdU) was given in an additional experiment to basic medium cultures, and incorporation was determined 12 h later by immunofluorescence (BrdU Labelling and Detection Kit I, Roche Diagnostic, Penzsberg, Germany). BrdU incorporation by Vero cells (ABAC, Buenos Aires, Argentina) incubated at 37 °C in D-MEM supplemented with 10% FCS and antibiotics was first tested as a positive control (data not shown).

Several media modifications were tested by comparing DNA content in cultures at 0 and 24 h ($n = 5$ per group) with a one-tailed Student's t-test. Results of supplementing the basic medium with fetal calf serum (and the corresponding controls) did not show a normal distribution (Kolmogorov–Smirnov test), but they did so after square root transformation.

In all cases, the quality of cultures was controlled through color changes in the culture medium (Phenol Red as pH indicator) and by observation in the inverted microscope for the presence of microorganism contamination. In one case the culture had to be discarded.

2.6. Short-term live cells time-lapse microscopy

Freshly withdrawn hemolymph (200 μL) was placed on a 35 mm glass coverslip. One millilitre of basic medium was added 15 min later (to allow cells to adhere before addition). The glass coverslip was placed in a temperature controlled chamber (28 °C) and
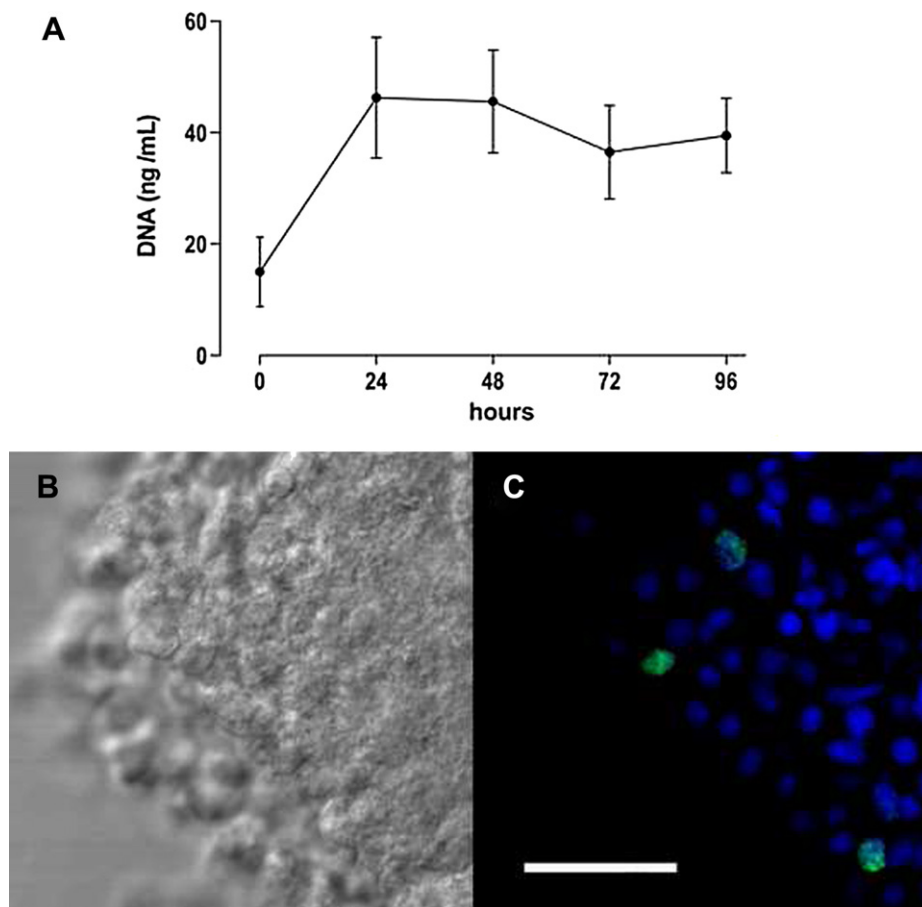

Fig. 2. A. Kinetics of *in vitro* growth of *Pomacea canaliculata* hemocytes (DNA ng/ml, mean ± SE of six independent experiments) during 0–96 h culture in the basic medium. Only the 0 h mean value differed from the other determinations (one-way ANOVA and Tukey test as *post hoc* analysis, $P < 0.05$). B. Periphery of a spheroidal aggregate, 12 h after seeding (phase contrast microscopy). C. Green immunofluorescence (BrdU) colocalizing with nuclear blue staining (Hoechst 33258) in the same aggregate shown in B (laser confocal microscopy). Scale bar = 50 μm. (For interpretation of the references to colour in this figure legend, the reader is referred to the web version of this article.)

observed with an inverted microscope (Nikon Eclipse TE-300). Time-lapse recordings were performed using NIS Elements D as acquisition software. An Andor™ Luca EM charge-coupled device camera captured 14-bit digital 1002–1004 pixels greyscale images every 60 s for 73 min.

2.7. Scanning electron microscopy

A similar amount of hemocytes was added to wells as described in Section 2.3, except that a plastic coverslip (Thermanox® Plastic Coverslip, Nunc™) was used instead of a glass one to cover the
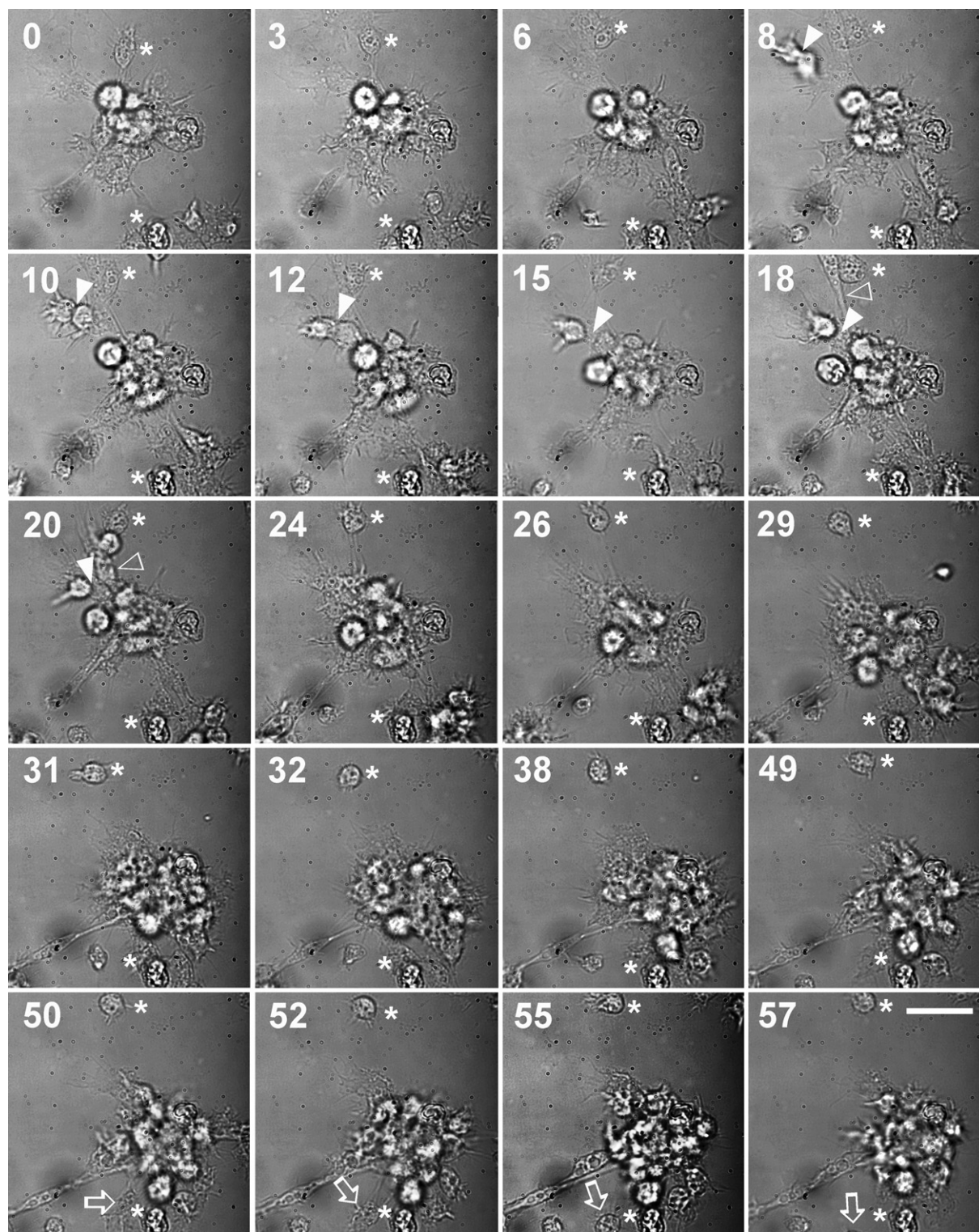

Fig. 3. Selected frames from time-lapse video microscopy showing the dynamics of early aggregate formation. Elapsed time in minutes is shown in the upper-left corner. Arrowheads indicate two cells together which are approximating the larger aggregate and finally merge with it (8–20 min). Open arrowheads show an elongated cell which rapidly joins the aggregate (18–20 min). Open arrows point to a cell which detaches from the aggregate and leaves the observation field (50–55 min). Also, a smaller cell aggregate appears in the lower right corner approximating the larger aggregate and finally joins with it (18–31 min). Asterisks indicate two cells which appear attached to the substrate and showed no apparent movements (0–57 min). Scale bar = 20 μm.

well's bottom. At 0, 24 and 96 h after seeding the plastic coverslip was removed and immersed in 2.5% glutaraldehyde for 30 min, and then the cells were gradually dehydrated in increasing ethanol concentrations (10−100% in distilled water), and then imbibed in 100% acetone before being critical point dried, gold coated on an aluminum stub, and viewed under a LEO 1450VP scanning electron microscope.

2.8. Dual DAPI/PI staining

Also, floating cell aggregates formed in culture were harvested and stained with 4′6′-diamidino-2-phenylindole (DAPI, 2.5 μg/mL) and propidium iodide (PI, 5 μg/mL) at room temperature for 15 min before being observed under the laser confocal microscope.

2.9. Transmission electron microscopy

Hemocytes were seeded in multiwell plates as described in Section 2.3 and floating spheroids which were formed in culture were removed by pipetting after 24−96 h, fixed in 4% paraformaldehyde−2.5% glutaraldehyde mixture and centrifuged. They were then dehydrated via graded ethanol solutions and embedded in Spurr's resin. Ultrathin sections (50−70 nm) were contrasted with aqueous uranyl acetate and lead citrate and observed under a Zeiss 900 transmission electron microscope.

2.10. Time course of hemocyte aggregation

In order to quantify the number of aggregates per mm^2 and the average area of aggregates at different times, hemocytes were cultured directly onto the culture dish as described in Section 2.3, and the experiment was repeated 6 times. Images were taken at 0, 4, 12, 24, 48, 72 and 96 h before seeding with an inverted microscope (Nikon Eclipse TE-300), using the same software and camera setting mentioned in Section 2.6. The aforementioned parameters were quantified using ImageJ software (NIH). Ten fields (1.54 mm^2) per time period were photographed to determine aggregate number. Also, the mean area of 100 aggregates was determined for each time period.

3. Results

3.1. Early hemocyte attachment, spreading and phagocytosis

Hemolymph obtained from the heart contained 2884 ± 419 cells/μL (mean ± SEM, $N = 20$), 9 ± 2% of which were eosinophilic granulocytes ($N = 10$). Freshly extracted hemolymph was used for seeding (200 μL per well) and for other microscopical observations.

When examined by scanning electron microscopy, cells had attached to the bottom as monolayers 15 min after seeding. About 60% appeared spreading star-shaped cells emitting long and thin filopodia (Fig. 1A) and most of them were interconnected (Figs. 1C and 5A−D).

No granulocytes remained attached to the coverslip after washing and fixation for laser confocal microscopy. Only 32−36% of the attached hyalinocytes showed phagocytosis of fluorescent latex beads within 4 h after seeding and this percentage did not change significantly during the studied period (ANOVA I; Fig. 1D). However, a small proportion of cells showed the ability to phagocytose more than 20 latex beads (Fig. 1C), and this percentage increased significantly during the studied period (from 4% at 1 h to 15% at 4 h; ANOVA I, followed by the Tukey test; Fig. 1D).

Formation of spheroidal aggregates had already begun in all cultures at the end of these observations (see Section 3.2.2).
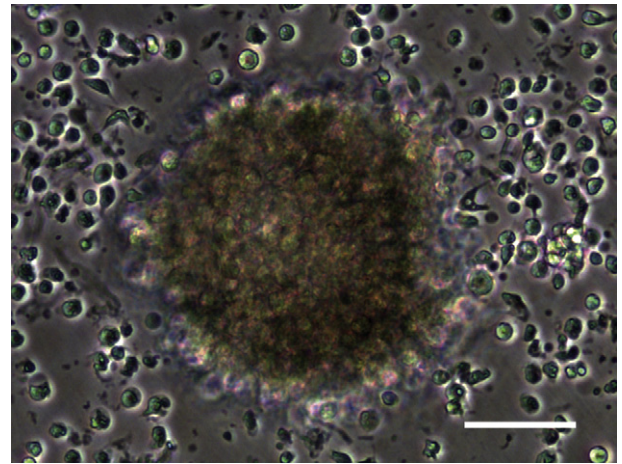

Fig. 4. A large multicellular spheroid, 24 h after seeding (bright field microscopy). Scale bar = 50 μm.

3.2. Hemocyte proliferation and aggregation in longer culture periods

3.2.1. Hemocyte growth in the basic medium and other supplemented or modified media

Cultures made both in the basic medium and in that supplemented with hemolymph plasma showed statistically significant increases in DNA concentration compared between 0 and 24 h after seeding. However, no significant increases were observed when the basic medium was supplemented with fetal calf serum or when the L-15 medium (diluted to match *P. canaliculata* plasma osmolality) was used (Supplementary figure 1).

After the initial 24 h DNA increase in the basic medium, the concentration did not changed significantly (Fig. 2A). BrdU incorporation 12 h after seeding was observed in cells within spheroids indicating cell proliferation (Fig. 2B and C).

3.2.2. Hemocyte spheroidal aggregates in culture

Time-lapse video microscopy showed the early aggregation of cells, 2 h after seeding. The incorporated cells arrived as floating round or spreading single cells (Fig. 3, 8−20 min). The initial contact between them was made by cellular extensions (Fig. 5C and D) and was followed by a rapid approach between cells (Fig. 3, 12−24 min). Also, merging of small cell aggregates was observed (Figs. 3 and 5E, 18−31 min). Nevertheless, this seems to be a dynamic process since outward migration of some cells could also be seen (Fig. 3, 50−57 min). The complete movie (60 min) corresponding to Fig. 3 is available as Supplementary material.

Supplementary video related to this article can be found at http://dx.doi.org/10.1016/j.fsi.2012.11.035.

Much larger spheroidal aggregates are formed later (Fig. 4). Under scanning electron microscopy, hemocytes were already attached to the bottom coverslip 15 min after seeding and many of them had become extremely flattened, star-shaped cells, emitting long filopodia with drumstick ends (Figs. 1A and 5A and D), while others were still rounded, 3−5 μm cells (Fig. 5A and B). Both cell types appeared emitting filopodia and/or lamellipodia (e.g., Fig. 5H).

Also under scanning electron microscopy, the cells began to form aggregates of irregular shape and surface within 24 h after seeding (Fig. 5E−H). In some cases, 2−3 aggregates appeared merging (Fig. 5E). Larger spheroidal aggregates (50−100 μm) with a smooth surface were seen 96 h after seeding (Fig. 5F and H). Numerous round cells, many of them emitting filopodia and lamellipodia, appeared either covering most of the aggregate's surface or in the bottom's surroundings (Fig. 5F and H). Indeed,
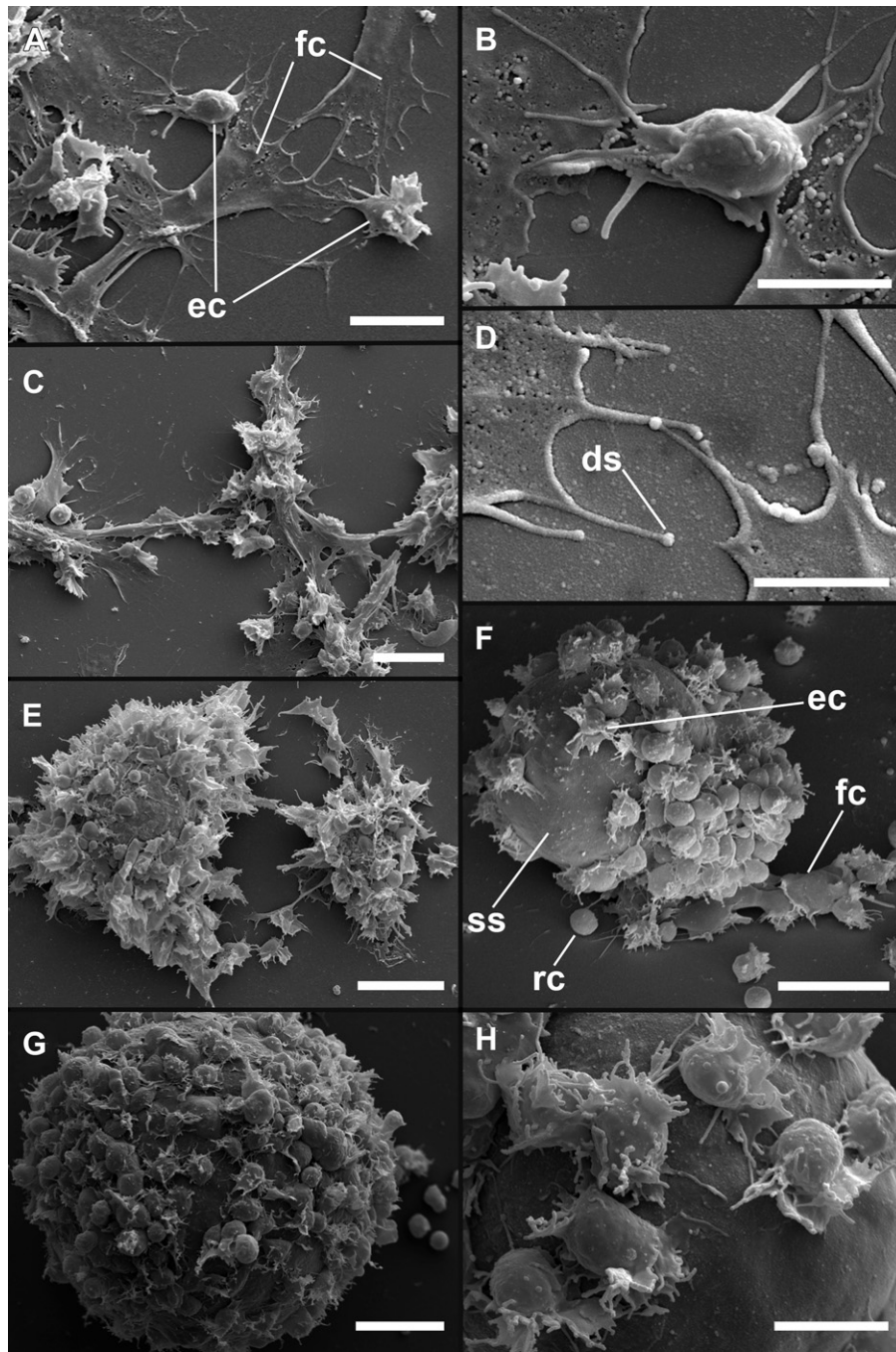
Fig. 5. Attached cells and aggregates (scanning electron microscopy). A. Hemocytes attached to the plastic bottom surface. Flattened cells (fc) and round filopodia/lamellipodia emitting cells (ec), 15 min after seeding; scale bar = 10 μm. B. Round cell emitting filopodia (detail from panel A); scale bar = 5 μm. C. Interacting flattened and some round, filopodia/lamellipodia emitting cells, 15 min after seeding; scale bar = 20 μm. D. High power magnification, showing the drumstick shaped ends (ds) of the filopodia of flattened cells, 15 min after seeding; scale bar = 3 μm. E. Merging cell aggregates, 24 h after seeding; numerous filopodia/lamellipodia emitting cells are seen on both aggregates; scale bar = 20 μm. F. Spheroidal aggregate partly covered by numerous filopodia/lamellipodia emitting cells; the stub was tilted 47° to show the aggregate's attachment to the bottom surface, where some flattened and round cells are also seen, 96 h after seeding; scale bar = 20 μm. G. Large spheroid mostly covered by filopodia/lamellipodia emitting cells, 96 h after seeding; scale bar = 20 μm. H. Detail of the smooth external aspect of a spheroid, with some filopodia–lamellipodia emitting cells on it, 96 h after seeding; scale bar = 20 μm. Abbreviations: ds, drumstick end; ec, filopodia/lamellipodia emitting cel; fc, flattened cell; rc, round cell; ss, smooth surface.

many of the latter cells appeared to be migrating to join the aggregates (e.g., Fig. 5F). The largest aggregates (above ∼120 μm in diameter) detached from the bottom surface and floated freely in the medium and so, they did not appear in scanning electron microscopy preparations.

The DAPI–PI staining of floating spheroids showed that these aggregates have a general organization including an outer cell layer, a region in which lacunae predominate, and an inner, more or less compact core. Much variable numbers of non-viable cells (marked in red), that are unable to exclude propidium iodide, were observed in different aggregates (Fig. 6).

Transmission electron microscopy of detached spheroidal aggregates was made 24–96 h after seeding, showing similar ultrastructural features throughout this period. In general, the aggregated hemocytes showed ovoid or elongated nuclei, with a dispersed chromatin matrix but also with some heavy
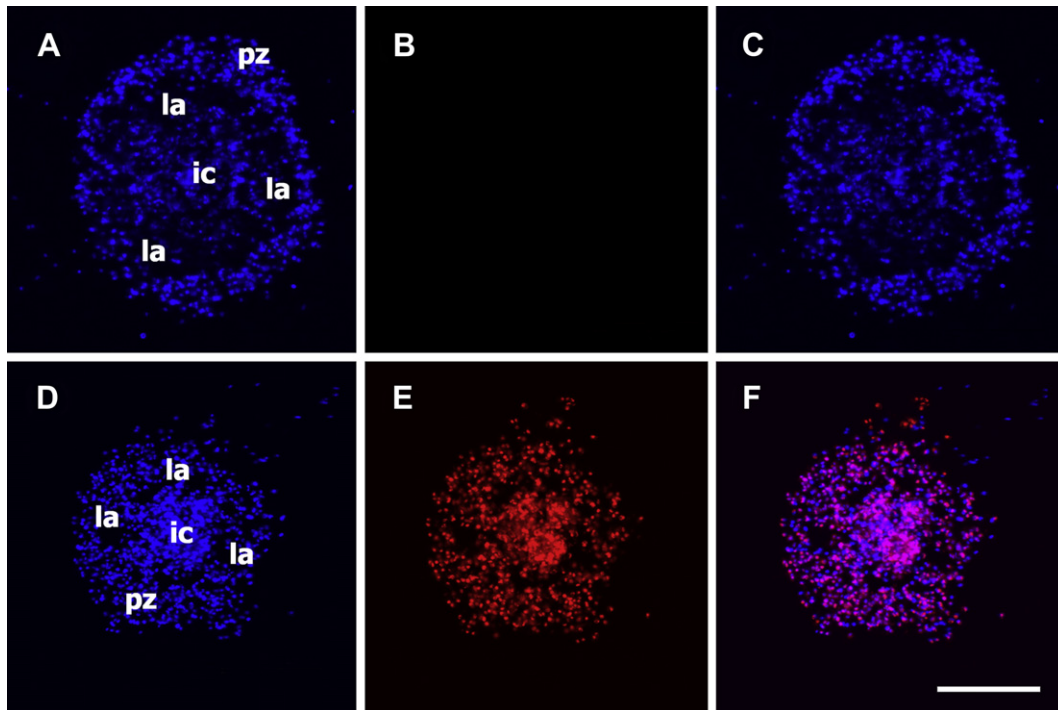
Fig. 6. Floating hemocyte aggregates, 72 h after seeding (DAPI and propidium iodide staining; laser confocal microscopy). A. Aggregate showing the peripheral cell zone, the intermediate lacunar zone and the inner core (ic) (DAPI emission, blue). B. Same aggregate lacking propidium iodide staining (red emission), indicating that all cells were viable. C. Merging of micrographs A and B. D. Another aggregate showing the same basic organization (DAPI emission, blue). E. Same aggregate showing abundant cells marked with propidium iodide (red emission), indicating that most cells in this aggregate were not viable. F. Merging of micrographs D and E. Abbreviations: ic, inner core; la, lacuna; pz, peripheral zone. Scale bar = 100 μm. (For interpretation of the references to colour in this figure legend, the reader is referred to the web version of this article.)

heterochromatic clumps and conspicuous nucleoli (Fig. 7A and B). Most cells are hyalinocytes, i.e., they do not contain large electron-dense granules, but do contain presumptive glycogen granules (Fig. 7A–C) as well as membrane bound areas containing phagocytized cellular remnants and 'myeloid' membrane profiles (Fig. 7D). The extracellular lacunae were numerous and were intercommunicating around the inner cell core, and contained a fibrillar material of moderate electron density (Fig. 7A and B).

The time course of cell aggregate formation was quantified both in terms of aggregate density (number of aggregates/mm^2) (Fig. 8A) and aggregate area (μm^2) (Fig. 8B) of the individual aggregates. Aggregate density peaked at 4 h after seeding and decreased thereafter, as a consequence of spheroid merging, which also resulted in an increasing mean area of the individual aggregates. In many cases, the three-layered organization of merged or unmerged spheroids was easily discernible by phase contrast microscopy (Fig. 8D). Spheroid merging cause aggregates to adopt capricious forms (Fig. 8E), and many of them become seen visible to the naked eye (they reach up to 1 mm^2).

4. Discussion

A culture medium was developed that allowed hemocytes to settle, attach, migrate and show phagocytosis of latex beads within 4 h after seeding. Afterwards, we were struck by the formation of spheroidal aggregates, which later detached from the substrate and even merged to form much larger aggregates. Aspects of hemocyte activity were examined at selected stages along this progression.

4.1. Initial attachment and spreading of hemocytes

Hemocytes of *P. canaliculata* were highly motile 15 min after seeding and were mostly flattened, spreading cells. However, and as it was recently reported for a bivalve mollusk [29], fast modifications of hemocyte shape, with bidirectional transitions from spreading to round cell outlines also occurred. In principle, active motility ensures a rapid scanning of large areas and hence, it increases the chance of contacting either foreign particles (to phagocytise) or other cells (to form aggregates, at least in the case of *P. canaliculata*). A direct correlation between vertebrate macrophage motility and phagocytic activity has been shown [30] and this has been implicated in immune surveillance *in vivo* against pathogen invasion [31].

4.2. Phagocytosis

Fluorescent particles were phagocytosed by hemocytes in a manner similar to that of other mollusks [e.g., 29,32]. Hemocyte exposure to fluorescent latex beads resulted in cell orientation towards the beads, and in switching from a symmetrical to a polarized cell shape, with the formation of lamellipodia at the cell's leading edge as do many vertebrate leukocytes [33–35]. Similar changes have also been shown in motile cells from several phylogenetically distant taxa [36–38], in agreement with the idea of an evolutionary conservation of these mechanisms.

In our experiments in *P. canaliculata*, all the attached hemocytes were hyalinocytes, and only 32–36% of them were able to engulf at least one latex bead, and the proportion of phagocytic cells did not change significantly during the studied period, which would indicate indeed that the phagocytic population is about one-third of circulating hyalinocytes. However, the percent of cells showing a greater phagocytic capacity (i.e., those engulfing 20 beads or more) increased up to 15% during the studied period, but it is still possible that this percent would have increased if the observations were continued for a longer time (this was not possible because of spheroid formation, that hampers these quantifications). Similar
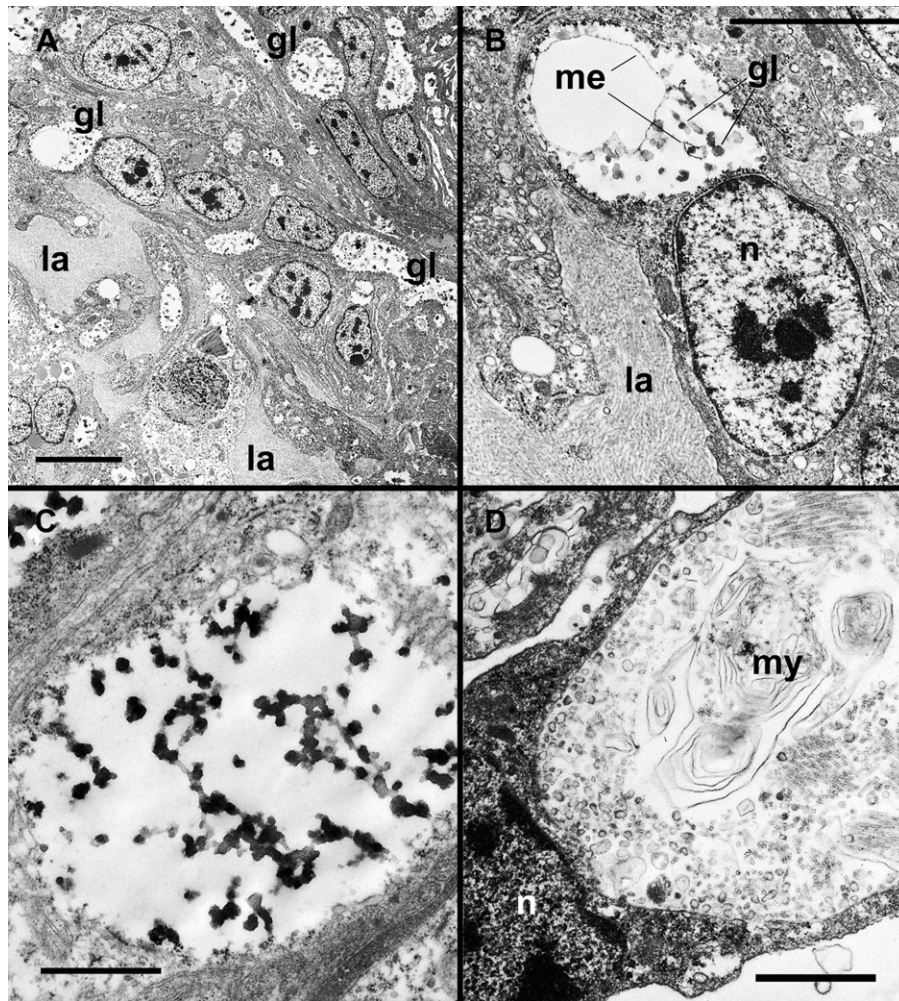
Fig. 7. Floating hemocyte aggregates (transmission electron microscopy). A. Cells bordering interconnected extracellular lacunae, and showing euchromatic nuclei with some heavy heterochromatic grains and nucleoli, and clear cytoplasmic areas with presumptive glycogen granules. The lacunae contain a fibrogranular material of moderate electron density; scale bar = 5 μm. B. Detail of nucleus of a cell shown in A, with heavy heterochromatic grains and a nucleolus; the fibrogranular material of the nearby lacuna is also seen; the cytoplasm shows an area with membrane remains and presumptive glycogen granules; scale bar = 1 μm. C. Detail of a membrane-unbound area with presumptive glycogen granules; scale bar = 1 μm. D. Detail of a cytoplasmic vesicle with 'myeloid figures'; scale bar = 1 μm. Abbreviations: gl, glycogen granules; la, lacuna; me, membrane remains; my, myeloid figures; n, nucleus.

percents of hemocytes phagocytosing at least a low number of beads were reported within 3 h after seeding in the vetigastropods *Haliotis tuberculata* [39], *Haliotis discus* and *Turbo cornutus* [40].

4.3. In vitro growth of circulating hemocytes

Hemopoietic organs have been described in pulmonate gastropods [41–43] and in *Marisa cornuarietis*, an ampullariid snail [44]. Hemocyte islets are also found in the kidney of *P. canaliculata* and they show phagocytic activity and spheroid formation after bacterial or yeast injections [24,45]. However, it has also been shown that hemocyte proliferation occurs in the circulation in littorinimorph and pulmonate gastropods [46–48], bivalves [49,50] and, although at low levels, in crustaceans [51–53]. The DNA increase and the BrdU incorporation in hemocyte primary cultures indicate that some cells with the ability to proliferate are found in the circulation of *P. canaliculata*.

4.4. Hemocyte spheroidal aggregates in culture

The formation of large spheroidal aggregates *in vitro* appears as a remarkable characteristic of *P. canaliculata*. Spheroids are found

since the first hours after seeding, and they grew in size during the subsequent days, during which many aggregates detach from the bottom coverslip and float freely in the medium. The aggregates showed some organization, including a compact core, an intermediate zone with large extracellular lacunae and an outer zone of flattened cells; and also, numerous round cells emitting cytoplasmic extensions were seen attaching to the spheroids' outer surface. Spheroids are composed by the non-granular hemocytes (mainly hyalinocytes) that account for 91% of circulating cells in *P. canaliculata*. As far as we know, the formation of such large spheroids by mollusk hemocytes has only been reported in a vetigastropod [18], an opisthobranch gastropod [54] and two bivalves [29,55]. Evidence of an internal organization of the spheroids has only been reported by Le Foll et al. [29] who showed a stratification of two types of hemocytes forming the spheroids in *Mytilus edulis*, but no indication of an internal organization has been previously reported in gastropod spheroids.

In *P. canaliculata*, the nuclei of cells in the spheroid's core and/or close to the extracellular lacunae are indicative of high transcriptional activity (a matrix of dispersed chromatin, heavy heterochromatic clumps and conspicuous nucleoli). Also, many clear, membrane-unbound areas in the cytoplasm contain small
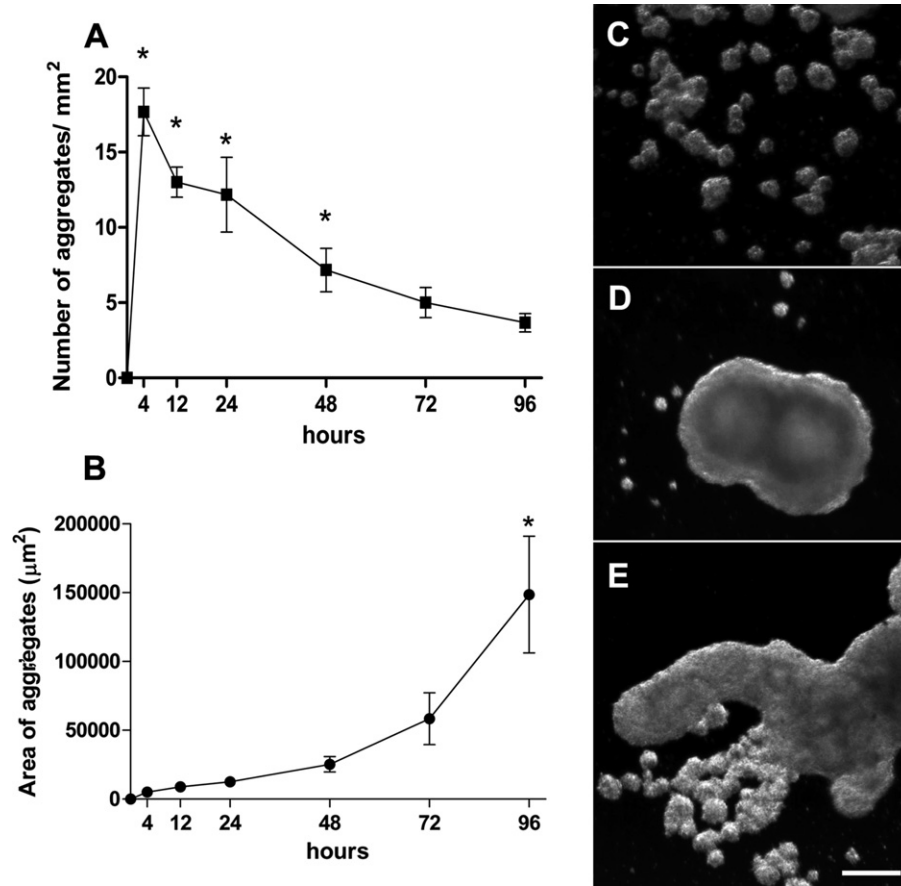
Fig. 8. Timing of aggregate formation in culture (asterisks indicate differences significantly different from zero; ANOVA I, Tukey test, $P < 0.05$). A. Aggregate density. B. Area of individual aggregates. C–E. Different degrees of aggregation (phase contrast, 96 h after seeding; scale bar = 200 μm).

electron-dense clumps in most hemocytes in the spheroids. These areas may be the result of merging of the small 'electron-lucid granules' reported by Shozawa and Suto [25] in circulating hemocytes of this species, which actually appeared in their micrographs as membrane-unbound areas which are likely to be glycogen deposits [56].

Dual DAPI/PI staining revealed that damaged cells (i.e., those with a membrane unable to exclude propidium iodide; [57]) also occur in a variable number within the spheroids. However, damaged cells were only infrequently found in them under transmission electron microscopy, which would indicate that propidium iodide was detecting cells in which membrane damage had not still resulted in recognizable ultrastructural changes or, alternatively, that dead cells are rapidly phagocytosed by living cells. In one way or the other, aggregates may be showing an equilibrium between cell proliferation and death, and this would explain the rather constant levels observed in DNA concentration from 24 to 96 h after seeding.

Time-lapse imaging revealed a remarkable migratory activity in the early phases of spheroid formation (2 h after seeding), with cells moving in and out of the aggregates. Also, rapid cell shape changes were observed, which indicate that round and flattened cells may not be alternative morphotypes, but the result of to and fro changes. Similarly, alternating spread and condensed phases of hemocyte shape have been reported in a bivalve [29].

4.5. Significance of cell aggregation and spheroid formation in mollusk and non-mollusk taxa

Hemocyte aggregation immediately after hemolymph withdrawal is a widespread mechanism in gastropods which may be significant for hemostasis in vivo [58] and they may also be involved in wound healing [59]. But larger spheroidal aggregations as those spontaneously formed by P. canaliculata hemocytes in vitro has been reported in at least four mollusk species [18,29,54,55] and a similar behavior has been reported in two decapod crustaceans [60]. However, the latter authors have also observed in vivo spheroid formation after bacterial injections in the hemocoel, and they have implicated spheroids in clearing of bacteria from the circulation [60]. In their study, spheroids were assumed to be stuck in the gill just because of the small size of vessels. Also, we have observed spheroid formation in the hemocyte kidney islets and in the lung of P. canaliculata after the injection of a yeast cell suspension in the visceral hump. The lung of P. canaliculata is an organ that does not normally show hemocyte islets as those of the kidney [45]. However, the lung spheroids do not seem primarily caused by trapping of hemocyte aggregates into the small vessels, since small- to medium-sized aggregates have also been observed within large vessels of this organ, even though they also extend into the smaller vessels and interstitial tissue of the lung. Further studies are needed to clarify the role of spheroids in the response to immune challenge in P. canaliculata as well as in other gastropods.

However, the formation of spheroidal aggregates after several hours in culture -instead of the more common formation of monolayers- may also be significant in a much wider context. Spheroid formation has been observed in cultures of several mammalian cancer cells [e.g., 61,62]. Spheroids from mammalian cells can also be prepared from non-tumoral cells, either in a single cell type suspension or in a mixture of several cell types, but only in permissive culture systems [63]. For instance, hepatocytes in such conditions first adhere to form a monolayer with spreading cell

morphology but, after 48 h of culture, they undergo contraction, migration, and transition from monolayer into spheroidal aggregates [64]. These structures are viewed as maintaining a tissue-like cytological structure which sustain higher levels of many differentiated functions than cells cultured as monolayers [63] and that they may bridge the gap between cell culture and live tissue [65]. Indeed, some form of cell organization has been shown in the spheroids formed by *P. canaliculata* hemocytes, and it is possible that the fibrillar material contained within the large extracellular lacunae found in spheroids were a kind of extracellular matrix, which may also play a role during *in vivo* wound healing; similarly, hemocyte participation in matrix deposition during tissue repair has been shown in arthropods and in a pulmonate gastropod [59,66].

Also, spheroids have gained special attention in biomedical research since they have been proposed as building blocks for tissue/organ bioengineering [63,67] and as tumor models in drug and radiotherapy research [65,68,69].

5. Conclusions

Circulating hemocytes from *P. canaliculata* have been cultured in a newly developed synthetic medium in which basic, evolutionary conserved behaviors such as attachment, spreading and phagocytosis could be studied.

However, the main finding of the current work is that hemocytes of *P. canaliculata* spontaneously form spheroidal aggregates during the first hours (and days) after seeding, instead of growing as monolayers. The spheroids do not appear as mere aggregates since they show a tridimensional organization. Also, numerous spheroids merge into large aggregates that may be visible with the naked eye. All these findings may be significant in the cellular immune response of this snail to microbial aggression, but also in a context wider than molluscan cell biology, including tumor biology and tissue bioengineering.

Acknowledgements

Appendix A. Supplementary data

Supplementary data related to this article can be found at http://dx.doi.org/10.1016/j.fsi.2012.11.035.

References

[1] Hayes KA, Cowie RH, Thiengo SC, Strong EE. Comparing apples to apples: clarifying the identities of two highly invasive Neotropical Ampullariidae. Zool J Linn Soc 2012;166:723–53.
[2] Cowie RH. Apple snails (Ampullariidae) as agricultural pests: their biology, impacts and management. In: Barker GM, editor. Molluscs as crop pests. Hamilton: CABI Publishing; 2002. p. 145–92.
[3] Hayes KA, Joshi RC, Thiengo SC, Cowie RH. Out of South America: multiple origins of non native apple snails in Asia. Divers Distrib 2008;14:701–12.
[4] Hayes KA, Cowie RH, Thiengo SC. A global phylogeny of apple snails: Gondwanan origin, generic relationships, and the influence of outgroup choice (Caenogastropoda: Ampullariidae). Biol J Linn Soc Lond 2009;98:61–76.
[5] Lv S, Zhou XN, Zhang Y, Liu HX, Zhu D, Yin WG, et al. The effect of temperature on the development of *Angiostrongylus cantonensis* (Chen 1935) in *Pomacea canaliculata* (Lamarck 1822). Parasitol Res 2006;99:583–7.
[6] Lv S, Zhang Y, Liu HX, Zhang CW, Steinmann P, Zhou XN, et al. *Angiostrongylus cantonensis*: morphological and behavioral investigation within the freshwater snail *Pomacea canaliculata*. Parasitol Res 2009;104:1351–9.
[7] Burela S, Martín PR. Nuptial feeding in the freshwater snail *Pomacea canaliculata* (Gastropoda: Ampullariidae). Malacologia 2007;49:465–70.
[8] Heras H, Frassa M, Fernández PE, Galosi CM, Gimeno EJ, Dreon MS. First egg protein with a neurotoxic effect on mice. Toxicon 2008;52:481–8.
[9] Dreon MS, Ituarte S, Heras H. The role of the proteinase inhibitor ovorubin in Apple snail eggs resembles plant embryo defense against predation. PLoS One 2010;5:e15059.
[10] Vega IA, Damborenea MC, Gamarra-Luques C, Koch E, Cueto JA, Castro-Vazquez A. Facultative and obligate symbiotic associations of *Pomacea canaliculata* (Caenogastropoda, Ampullariidae). Biocell 2006;30:367–75.
[11] Castro-Vazquez A, Albrecht EA, Vega IA, Koch E, Gamarra-Luques C. Pigmented corpuscles in the midgut gland of *Pomacea canaliculata* and other Neotropical apple-snails (Prosobranchia, Ampullariidae): a possible symbiotic association. Biocell 2002;26:101–9.
[12] Cooper MD, Alder MN. The evolution of adaptive immune systems. Cell 2006; 124:815–22.
[13] Salzet M. Vertebrate innate immunity resembles a mosaic of invertebrate immune responses. Trends Immunol 2001;22:285–8.
[14] Hartenstein V. Blood cells and blood cell development in the animal kingdom. Annu Rev Cell Dev Biol 2006;22:677–712.
[15] Bayne CJ. Phagocytosis and non-self recognition in invertebrates. BioScience 1990;40:723–31.
[16] Ottaviani E. Molluscan immunorecognition. Invertebr Surviv J 2006;3:50–63.
[17] Lebel JM, Giard W, Favrel P, Boucaud-Camou E. Effects of different vertebrate growth factors on primary cultures of hemocytes from the gastropod mollusc, *Haliotis tuberculata*. Biol Cell 1996;86:67–72.
[18] Auzoux-Bordenave S, Fouchereau-Peron M, Helleouet MN, Doumenc D. CGRP regulates the activity of mantle cells and hemocytes in abalone primary cell cultures (*Haliotis tuberculata*). J Shellfish Res 2007;26:887–94.
[19] Barbosa L, Silva LM, Coelho PMZ, Santos SR, Fortes-Dias CL. Primary culture of the region of the amebocyte-producing organ of the snail *Biomphalaria glabrata*, the intermediate host of *Schistosoma mansoni*. Mem Inst Oswaldo Cruz 2006;101:639–43.
[20] Adema CM, Harris RA, van Deutekom-Mulder EC. A comparative study of hemocytes from six different snails: morphology and functional aspects. J Invertebr Pathol 1992;59:24–32.
[21] Mahilini HM, Rajendran A. Categorization of hemocytes of three gastropod species *Trachea vittata* (Muller), *Pila globosa* (Swainson) and *Indoplanorbis exustus* (Dehays). J Invertebr Pathol 2008;97:20–6.
[22] Ottaviani E, Franchini A. Ultrastructural study of haemocytes of the freshwater snail *Planorbarius corneus* (L.) (Gastropoda, Pulmonata). Acta Zool 1988;69:157–62.
[23] Furuta E, Yamaguchi K, Shimozawa A. The ultrastructure of hemolymph cells of the land slug, *Incilaria fruhstorferi* Collinge (Gastropoda: Pulmonata). Anat Anz 1986;162:215–24.
[24] Cueto JA. *Pomacea canaliculata* (Architaenioglossa, Ampullariidae): La hemolinfa y sus células. Mendoza: Universidad Nacional de Cuyo; 2011.
[25] Shozawa A, Suto C. Hemocytes of *Pomacea canaliculata*: I. Reversible aggregation induced by Ca^{2+}. Dev Comp Immunol 1990;14:175–84.
[26] Cueto JA, Fogal T, Castro-Vazquez A. Ultrastructural characterization of circulating hemocytes of *Pomacea canaliculata*. Biocell 2007;32:103 [abstract].
[27] Giraud-Billoud M, Koch E, Vega IA, Gamarra-Luques C, Castro-Vazquez A. Urate cells and tissues in the South American apple snail *Pomacea canaliculata*. J Molluscan Stud 2008;74:259–66.
[28] Labarca C, Paigen K. A simple, rapid and sensitive DNA assay procedure. Anal Biochem 1980;102:344–52.
[29] Le Foll F, Rioult D, Boussa S, Pasquier J, Dagher Z, Leboulenger F. Characterisation of *Mytilus edulis* hemocyte subpopulations by single cell time-lapse motility imaging. Fish Shellfish Immunol 2010;28:372–86.
[30] Neta R, Salvin SB. Cellular immunity *in vitro*: migration inhibition and phagocytosis. Infect Immun 1971;4:697–702.
[31] Sánchez-Madrid F, del Pozo MA. Leukocyte polarization in cell migration and immune interactions. EMBO J 1999;18:501–11.
[32] Mortensen SH, Glette J. Phagocytic activity of scallop (*Pecten maximus*) haemocytes maintained *in vitro*. Fish Shellfish Immunol 1996;6:111–21.
[33] Howard TH, Oresajo CO. The kinetics of chemotactic peptide-induced change in F-actin content, F-actin distribution, and the shape of neutrophils. J Cell Biol 1985;101:1078–85.
[34] Coates TD, Watts RG, Hartman R, Howard TH. Relationship of F-actin distribution to development of polar shape in human polymorphonuclear neutrophils. J Cell Biol 1992;117:765–74.
[35] del Pozo MA, Sánchez-Mateos P, Nieto M, Sánchez-Madrid F. Chemokines regulate cellular polarization and adhesion receptor redistribution during lymphocyte interaction with endothelium and extracellular matrix. Involvement of cAMP signaling pathway. J Cell Biol 1995;131:495–508.
[36] Hotulainen P, Lappalainen P. Stress fibers are generated by two distinct actin assembly mechanisms in motile cells. J Cell Biol 2006;173:383–94.
[37] May RC, Machesky LM. Phagocytosis and the actin cytoskeleton. J Cell Sci 2001;114:1061–78.
[38] Aderem A, Underhill DM. Mechanisms of phagocytosis in macrophages. Annu Rev Immunol 2003;17:593–623.
[39] Travers M, Mirella da Silva P, Le Go c N, Marie D, Donval A, Huchette S, et al. Morphologic, cytometric and functional characterisation of abalone (*Haliotis tuberculata*) haemocytes. Fish Shellfish Immunol 2008;24:400–11.
[40] Donaghy L, Hong H, Lambert C, Park H, Shim W, Choi K. First characterisation of the populations and immune-related activities of hemocytes from two edible gastropod species, the disk abalone, *Haliotis discus discus* and the spiny top shell, *Turbo cornutus*. Fish Shellfish Immunol 2010;28:87–97.

[41] Jeong KH, Lie KJ, Heyneman D. The ultrastructure of the amoebocyte-producing organ in *Biomphalaria glabrata*. Dev Comp Immunol 1983;7:217—28.

[42] Rondelaud D, Barthe D. Relationship of the amebocyte-producing organ with the generalized amoebocytic reaction in *Lymnaea truncatula* Muller infected by *Fasciola hepatica* L. Int J Parasitol 1982;68:967—9.

[43] Lie KJ, Heyneman D, Yau P. The origin of ameobocytes in *Biomphalaria glabrata*. J Parasitol 1975;63:574—6.

[44] Yousif F, Blähser S, Lämmler G. The cellular responses in *Marisa cornuarietis* experimentally infected with *Angiostrongylus cantonensis*. Parasitol Res 1980; 62:179—90.

[45] Rodríguez C, Vega IA, Cueto JA, Castro-Vazquez A. Hemocyte spheroidal aggregates in the kidney and lung of the Apple-snail (*Pomacea canaliculata*) after an immune challenge. Biocell 2012;36. [abstract].

[46] Sminia T. Haematopoiesis in the freshwater snail *Lymnaea stagnalis* studied by electron microscopy and autoradiography. Cell Tissue Res 1974;150:443—54.

[47] Sminia T, Van der Knaap W, Van Asselt L. Blood cell types and blood cell formation in gastropod molluscs. Dev Comp Immunol 1983;7:665—8.

[48] Gorbushin AM, Iakovleva NV. Haemogram of *Littorina littorea*. J Mar Biol Assoc UK 2006;86:1175—81.

[49] Matozzo V, Marin MG, Cima F, Ballarin L. First evidence of cell division in circulating haemocytes from the Manila clam *Tapes philippinarum*. Cell Biol Int 2008;32:865—8.

[50] Mayrand E, St-Jean SD, Courtenay SC. Haemocyte responses of blue mussels (*Mytilus edulis* L.) transferred from a contaminated site to a reference site: can the immune system recuperate? Aquac Res 2005;36:962—71.

[51] Söderhäll I, Bangyeekhun E, Mayo S, Söderhäll K. Hemocyte production and maturation in an invertebrate animal; proliferation and gene expression in hematopoietic stem cells of *Pacifastacus leniusculus*. Dev Comp Immunol 2003;27:661—72.

[52] Sequeira T, Tavarest D, Arala-Chaves M. Evidence for circulating hemocytes proliferation in the shrimp *Penaeus japonicus*. Dev Comp Immunol 1996;20: 97—104.

[53] Gargioni R, Barracco MA. Hemocytes of the palaemonids *Macrobrachium rosenbergiiand*, *M. acanthurus* and of the Penaeid *Penaeus paulensis*. J Morphol 1998;236:209—21.

[54] Martin GG, Oakes CT, Tousignant HR, Crabtree H, Yamakawa R. Structure and function of haemocytes in two marine gastropods, *Megathura crenulata* and *Aplysia californica*. J Molluscan Stud 2007;73:355—65.

[55] Wang Y, Hu M, Chiang MWL, Shin PKS, Cheung SG. Characterization of subpopulations and immune-related parameters of hemocytes in the green-lipped mussel *Perna viridis*. Fish Shellfish Immunol 2012;32:381—90.

[56] Revel JP, Napolitano L, Fawcett DW. Identification of glycogen in electron micrographs of thin tissue sections. J Biophys Biochem Cytol 1960;8:575—89.

[57] Sasaki DT, Dumas SE, Engleman EG. Discrimination of viable and non viable cells using propidium iodide in two color immunofluorescence. Cytometry 1987;8:413—20.

[58] Voltzow J. Gastropoda: Prosobranchia. In: Harrison FW, Kohn AJ, editors. Microscopic anatomy of invertebrates. New York: Wiley-Liss; 1994. p. 111—252.

[59] Franchini A, Ottaviani E. Repair of molluscan tissue injury: role of PDGF and TGF-b1. Tissue Cell 2000;32:312—21.

[60] Martin GG, Kay J, Poole D, Poole C. In vitro nodule formation in the ridgeback prawn, *Sicyonia ingentis*, and the American lobster, *Homarus americanus*. Invertebr Biol 1998;117:155—68.

[61] Dardousis K, Voolstra C, Roengvoraphoj M, Sekandarzad A, Mesghenna S, Winkler J, et al. Identification of differentially expressed genes involved in the formation of multicellular tumor spheroids by HT-29 colon carcinoma cells. Mol Ther 2007;15:94—102.

[62] Kelm JM, Timmins NE, Brown CJ, Fussenegger M, Nielsen LK. Method for generation of homogeneous multicellular tumor spheroids applicable to a wide variety of cell types. Biotechnol Bioeng 2003;83:173—80.

[63] Lin RZ, Chang HY. Recent advances in three-dimensional multicellular spheroid culture for biomedical research. Biotechnol J 2008;3:1172—84.

[64] Tzanakakis ES, Hansen LK, Hu WS. The role of actin filaments and microtubules in hepatocyte spheroid self-assembly. Cell Motil Cytoskeleton 2001;48: 175—89.

[65] Pampaloni F, Reynaud EG, Stelzer EHK. The third dimension bridges the gap between cell culture and live tissue. Nat Rev Mol Cell Biol 2007;8:839—45.

[66] Theopold U, Schmidt O, Soderhall K, Dushay MS. Coagulation in arthropods, defence, wound closure and healing. Trends Immunol 2004;25:289—94.

[67] Mironov V, Visconti RP, Kasyanov V, Forgacs G, Drake CJ, Markwald RR. Organ printing: tissue spheroids as building blocks. Biomaterials 2009;30:2164—74.

[68] Dubessy C, Merlin JL, Marchal C, Guillemin F. Spheroids in radiobiology and photodynamic therapy. Crit Rev Oncol Hematol 2000;36:179—92.

[69] Desoize B, Jardillier JC. Multicellular resistance: a paradigm for clinical resistance? Crit Rev Oncol Hematol 2000;36:193—207.